Influence of pore fluid-soil structure interactions on compacted lime-treated silty soil

Geetanjali Das, Andry Razakamanantsoa, Gontran Herrier, Dimitri Deneele

Influence of pore fluid-soil structure interactions on compacted lime-treated silty soil

Geetanjali Das[a,*], Andry Razakamanantsoa[a], Gontran Herrier[b], Dimitri Deneele[a,c]

[a]*GERS-GIE, Université Gustave Eiffel, IFSTTAR, F-44344 Bouguenais, France*

[b]*Lhoist Recherche et Développement, rue de l'Industrie 31, 1400 Nivelles, Belgique*

[c]*Université de Nantes, CNRS, Institut des Matériaux Jean Rouxel, IMN, F-44000 Nantes, France*

Post-print published in Engineering geology, 296(2022) https://doi.org/10.1016/j.enggeo.2021.106496

Highlights

- Kneading-and static-compacted soil is percolated by demineralized water and a low-ionic strength solution.
- Kneading action increases hydraulic tortuosity and pore fluid-soil structure contact.
- Effect of pore-fluid nature is more pronounced in kneaded soil than statically compacted soil.
- Demineralized water is relatively aggressive and enhances the leaching of lime.
- Pore volume flow is an important index to assess the durability of a hydraulic structure.

Abstract

The effects on hydromechanical performance due to chemical interactions between pore solution and soil components in lime-treated soil are investigated. Static- and kneading-compacted soils are percolated by demineralized water (DW) and a low-ionic strength solution. Kneading action causes aggregate deformation, thus consequently reducing macropores of diameter 10^5 Å. This increases the hydraulic tortuosity and lengthens the pore fluid-soil structure contact, which favors the long-term pozzolanic reactions. DW being relatively more aggressive than low-ionic strength solution accelerates the leaching of Calcium, thus negatively impacting the hydromechanical performance. The study shows that the hydromechanical evolution in lime-treated soil is governed by the duration of pore fluid and soil structure contact, depending on the compaction mechanisms implemented. The extent of the effect of pore fluid-soil structure interaction is regulated by the pore solution chemistry and the lime content. Thus, importance should be given to the relevancy of the selected compaction procedure and the permeant solution at the laboratory scale with respect to in-situ compaction mechanism and pore water.

Keywords: lime-treated soil; kneading action; pore fluid; tortuosity; leaching.

1. Introduction

Soil stabilization is a current practice for the efficient and effective management of natural resources in any land and infrastructure development project. The process of soil stabilization involves two main categories: mechanical improvement and chemical stabilization (Houben and Guillaud, 1994). Mechanical improvement involves the use of proper implementation techniques such as proper mixing of soil with chemical binder and water, compaction of soil through a suitable mechanism, and at an appropriate water content and compaction energy (le Runigo et al., 2011, 2009; Little, 1987). Chemical stabilization consists of the use of inorganic or organic binders, such as slags (Poh et al., 2006; Wild et al., 1998), fly ashes produced from coal-burning (Kolias et al., 2005; Show et al., 2003), cement kiln dust (Miller and Azad, 2000), and lime (Akula et al., 2020; Ali and Mohamed, 2019; Das et al., 2020; 2021; Makki-Szymkiewicz et al., 2015).

Lime is one of the most versatile (Dowling et al., 2015), low-cost (Inkham et al., 2019), and readily available chemicals. It was shown to be paramount in several applications using environmentally friendly techniques (Dowling et al., 2015). Soil treated by lime can be used repeatedly, thus promoting its reuse and improving cost-effectiveness (Hopkins et al., 2007). Upon mixing soil with lime, two effects are observed: (i) instant reduction in moisture content and consequent flocculation/agglomeration of the clay particles, further lowering soil plasticity and increasing workability of the lime-treated soil (Bell, 1996; Diamond and Kinter, 1965; Little, 1995, 1987); (ii) long-term increase in strength of the lime-treated soil due to the formation of cementitious compounds coming mainly from pozzolanic reactions (Das et al., 2020; Lemaire et al., 2013; Pu et al., 2019; Verbrugge et al., 2011).

Several laboratory studies and few field studies are available that explain the importance of the hydromechanical performances of the lime-treated soil towards the maintenance of the long-term durability of lime-treated earth structures (Das et al., 2020; 2021; Deneele et al., 2016; le Runigo et al., 2011, 2009; Lemaire et al., 2013; Verbrugge et al., 2011). The hydromechanical behavior is heavily influenced by compaction conditions such as compaction procedure, energy, and water content (Cuisinier et al., 2011; le Runigo et al., 2009; Mitchell et al., 1965; Watabe et al., 2000), which plays a central role in the mechanical improvement process. According to le Runigo et al. (2011, 2009) and Mitchell et al. (1965), lime-treated soil compacted at different initial moisture contents and compaction energies shows different magnitudes of hydraulic conductivity, k. This is because the hydraulic conductivity of soil depends on the macropore structure of the soil, which was shown to be a direct function of compaction conditions by Ranaivomanana

et al. (2018, 2017). A higher magnitude of k indicates a greater quantity of water percolation throughout the compacted soil in a short time. This can enhance the leaching of cementitious compounds as well as the available lime, which consequently decreases the compressive strength of the lime-treated soil, as reported by Le Runigo et al. (2011) and Deneele et al. (2016).

Although the consideration of moisture content and the implemented energy during compaction were shown to have a significant impact on the hydromechanical evolution, how well the laboratory-implemented compaction mechanism represents the in-situ compaction mechanism is an important question. In-situ fine-grained soil is often compacted by a pad foot roller, especially hydraulic earthen structures (dikes, levees, dams, reservoirs). The pad-foot roller often consists of pads attached to the drum surface of the wheel. During compaction, these pads generate a kneading action in the soil. The impact of kneading action in natural soil was evaluated by Kouassi et al. (2000), who demonstrated an equivalent generation of soil characteristics such as dry density and elastic stiffness between laboratory and field compacted soil. A similar observation was also reported by Clegg, (1964). Cuisinier et al. (2011) evaluated the evolution of hydraulic properties of lime-treated soil compacted by two procedures: static and kneading. A lower k was observed in the lime-treated kneaded soil. Beyond these few studies, further evaluation of the kneading mechanism, particularly with respect to lime-treated fine-grained soil, remains less investigated. Thus, it is reasonable to investigate the influence of the kneading mechanism in the hydromechanical evolution of lime-treated soil.

Another essential aspect that has remained less investigated with respect to the hydromechanical evaluation is the effect of the chemistry of pore water solution during its percolation through lime-treated compacted soil. Since lime-treated soil is susceptible to increased leaching, it may cancel out the improvement brought by lime treatment (Deneele et al., 2016). Hence, the leaching mechanism of lime-treated soil should be evaluated by considering the chemistry of porewater to which the selected soil is subjected to. The effect of the chemistry of pore fluid such as leachates on the hydraulic behavior of natural clay in the context of liner material used in underground nuclear disposal repository was widely investigated. Several studies have shown how the aggressive effect of leachates induces cracks in clay-liner and causes an increased hydraulic conductivity during the soil-leachate interactions (He et al., 2015; Sunil et al., 2008; Vaverková et al., 2020). Currently, DW is used as a conventional permeant solution in most of the existing studies to investigate the hydraulic and leaching behaviors of lime-treated soil, whereas in the field, water from natural sources influences such behaviors. Thus, it is essential to consider the interactions of pore solution chemistry with the lime-treated soil while investigating the soil's hydromechanical evolution.

In this context, the present study investigates the influence of compaction modes and pore solution chemistry on the hydromechanical performances of a lime-treated silty soil. The compaction modes

involved static and kneading compactions, and DW and a low ionic strength solution were used as pore solutions. The investigation includes evaluating the hydraulic conductivity and mechanical performances based on the leaching mechanism and microstructural modifications.

2. Materials and Methodologies

2.1. Soil, Lime, and permeant solutions properties

The soil selected in this study was silty soil imported from Marche-Les-Dames (Belgium). The main geotechnical properties of the soil were obtained from the studies reported by Charles et al. (2012) and Makki-Szymkiewicz et al. (2015). The soil is composed of 12% clay and 82% silt fraction. Its liquid limit is 31%, and the plasticity index is between 8 to 12. The Methylene blue value is 2.5 g/100 g. The mineralogy of the soil consists of Illite, Kaolinite, and Chlorite as clay minerals along with Quartz and Feldspars.

The quicklime (CaO) used for the treatment was supplied by Lhoist. The lime consists of 90.9% of available CaO and a reactivity (t_{60}) of 3.3 min. The Lime Modification Optimum (LMO) of the silt, which defines the minimum lime content required to initiate the pozzolanic reactions, was determined by Eades and Grim, (1966). The LMO was found to be 1% by weight of lime. Three different lime contents were used, lime content equal to LMO, 2.5%, and 4%.

Two permeant solutions were chosen DW, and DW+10^{-3}M NaCl. The latter has been used previously by Razakamanantsoa and Djeran-Maigre (2016) and Sato et al. (2017) as a reference fluid to highlight the negative effect of leachates on Bentonites in the context of landfill. The pH and Electric Conductivity (EC) of the DW and DW+10^{-3} M NaCl, latter regarded as Low-mineralized Water (LW) is presented in Table 1.

Table 1

The pH and Electric Conductivity of solutions

Permeant solutions	pH	Electric Conductivity (µS/cm)
DW	7.4	4.0
LW	6.5	172.0

2.2. Sample preparations

The maximum dry density, $\rho_{d(max)}$, and Optimum Moisture Content (OMC) of the untreated and the 3 different lime-treated silt were obtained by standard Proctor test as per ASTM, D698-12e2 and are presented in Table. 2.

Table 2

Maximum dry density and OMC of untreated and lime-treated silty soil

Soil	$\rho_{d(max)}$ (kN/m^3)	OMC (%)
Untreated silty soil	18.4	14.3
Silty soil treated with 1% lime	17.4	17.6
Silty soil treated with 2.5% lime	17.1	18.5
Silty soil treated with 4% lime	17.0	18.7

The silt was air-dried, sieved, and was then mixed with distilled water at OMC. The soil mixture was stored in sealed plastic bags for about 24 hours to allow moisture content homogenization. The wet soil and the respective lime were then mixed and were rested for 1 hour before compaction.

Cylindrical specimens of dimensions 0.05 m in height and 0.05 m diameter were prepared by Static (S) and Kneading (K) compaction methods at the constant compaction parameters mentioned in Table 2.

The static compaction involves compression of the specimens from top and bottom, as demonstrated by Holtz et al. (1981). The kneading compaction was performed by a laboratory-developed kneading tool. The process of kneading compaction was conducted, as demonstrated by Kouassi et al. (2000) for natural soil. Kouassi et al. (2000) does not consider compaction energy during kneading compaction, whereas, in the present study, compaction energy corresponding to the one mentioned in ASTM D698-91 was applied for specimens preparation. The application of the compaction load was made successively with the rotation of the 3-kneading feet by an angle of 45° between 2 successive loadings.

A total of 18 specimens was prepared, 9 specimens corresponding to each compaction method. After compaction, specimens were wrapped in plastic film and cured for 28-days at a laboratory temperature of 20 ± 1 ˚C.

2.3. Laboratory tests

2.3.1. Hydraulic conductivity test

2.3.1.1. Percolation setup

Hydraulic conductivity test was performed with flexible wall permeameter by a constant hydraulic head. The percolation system established was similar to the one used by Ranaivomanana et al. (2017). A schematic design of the permeability setup is presented in Fig. 1.

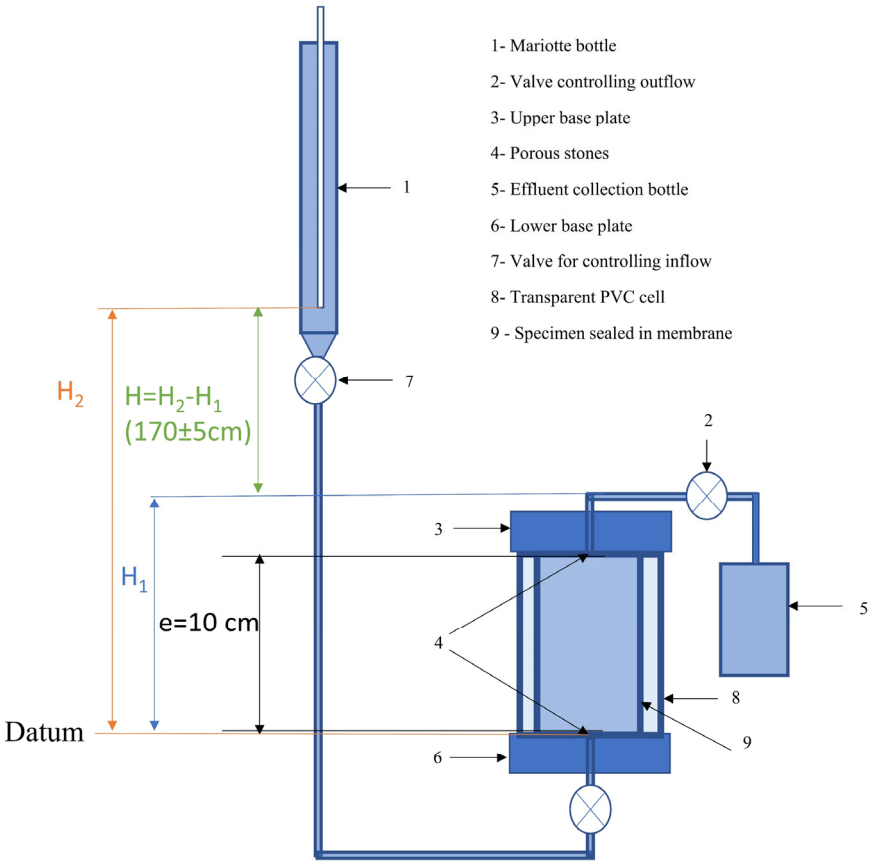

Fig. 1 Schematic diagram of flexible wall permeameter setup (*Dimensions are not as per scale*)

At the end of the curing time, specimens were sealed in a cellulose membrane and placed inside cylindrical transparent Polyvinyl chloride (PVC) cell with porous stones on its top and bottom (Fig. 1). A water inlet valve was equipped at the center of the PVC cell for applying the confining stress. The PVC cell, along with the membrane and specimen, was then placed within an upper and a lower base plate to avoid vertical deformation. Both the base plate are accompanied by a hole at its center for allowing outflow and inflow of solution in and from the specimen, respectively. The valve connected to the hole at the lower base plate was linked with the Mariotte bottle (Fig. 1). During the hydraulic test, the solution from the Marriott bottle passes through the base of the specimen. This is to ensure uniform flow throughout the

specimen by reducing any presence of entrapped air within the compacted specimen. The percolated fluid was collected in an effluent collection bottle linked with the valve connected to the hole in the upper base plate (Fig. 1).

A total of 12 setups for hydraulic conductivity tests were designed, of which 6 setups consist of specimens submitted to DW, and the remaining were submitted to LW.

2.3.1.2. Hydraulic conductivity test protocol

During the hydraulic conductivity test, a confining pressure of 88±2 kPa was applied for at least 24-48 hours before the application of hydraulic head pressure to ensure the homogeneity of the stress distribution. The hydraulic head applied (H) was 170±5 cm. Thus, the applied confining stress was about 5 times higher than the hydraulic head pressure. This was done (i) to maintain the structure of the compacted specimen against any microstructure change due to the hydraulic head, and (ii) to avoid any preferential flow between the soil and the membrane (Ranaivomanana et al., 2017).

The hydraulic conductivity test was conducted in accordance with the flow conditions provided by Darcy's law. According to Darcy, the hydraulic conductivity, k (m/s) in terms of the total discharge, $Q = dV/dt$, through a specimen; the cross-sectional area of the flow, A (m^2); and the hydraulic gradient, $i = H/e$ can be expressed as follows (Equation 1).

$$k = \frac{dV * e}{dt * A * H} \quad (1)$$

where $H=H_2-H_1$ is the hydraulic head (elevation datum) in m, and e is the specimen thickness in m; dV is the incremental volume of percolated water between two measurements in m^3; dt is the time elapsed between two measurements in seconds.

The hydraulic conductivity test was carried out in two phases: saturation and percolation. The saturation phase involves the wetting of specimens until full saturation, and the percolation phase involves the renewal of the entire porewater in the specimens. During the saturation phase, the outlet of the permeability setup was kept closed until a volume of influents corresponding to 1 Pore Volume Flow (PVF) of each specimen enter the specimens. One PVF is defined as the volume of pore water required to fill and renew the total volume of pore water and void initially present in the soil once (Katsumi et al., 2008). This level of PVF was selected to ensure about 90-95% saturation of the specimens before initiating the percolation phase. Mathematically, 1 PVF is the product of the volume of soil solids, $V_{s,}$ and the void ratio,

202 *e* of a given specimen. Then the accumulated volume of flow passing through the soil is denoted in terms
203 of PVF by dividing the total flow by the volume corresponding to 1 PVF.
204 The concept of PVF was proposed to consider the duration of contact between the permeant
205 solution and the lime-treated soil. Longer contact between soil and the permeant solution might be favorable
206 to the development of dissolution or precipitation mechanism inside the soil structure. Thus, the PVF can
207 be called an important index to assess the durability of the lime treatment. PVF was less often used for
208 hydraulic performance studies related to lime-treated soil. However, it was widely implemented in the
209 literature related to the hydraulic performance of Bentonite used in waste storage management (Katsumi et
210 al., 2008; Shackelford et al., 2000).
211 The hydraulic conductivity measurements were stopped in accordance with the following
212 termination criteria: (i) after 40 PVF was reached; and (ii) the last 5 values of EC measured during
213 percolation became almost stable. Such termination criteria were also referred to in a study reported by
214 Shackelford et al. (2000).
215
216 *2.3.1.3. Calcium analysis*
217 During the percolation phase, effluents were collected at different PVF. The effluents were then
218 filtered using 0.45 µm syringe prior to Inductively Coupled Plasma Optical Emission Spectrometry (ICP
219 OES) analysis for determining the elementary concentrations of Calcium (*Ca*). The analysis of *Ca*
220 concentration was made to investigate the difference in the concentration of *Ca* leached from the lime-
221 treated soil under the influence of DW and LW.
222
223 *2.3.2. Unconfined compressive strength (UCS) test*
224 Specimens after 28 days of curing and at the end of the percolation phase were subjected to
225 compressive strength analysis using a mechanical press with a load sensor of 10 kN. The load was applied
226 to the specimens at a constant axial displacement rate of 1 mm/min.

227 *2.3.3. Pore structure determination*
228 Soil specimens sampled from 28 days cured soil and from specimens at the end of hydraulic
229 conductivity test were freeze-dried and then subjected to Mercury Intrusion Porosimetry (MIP) test using
230 Micromeritics Auto Pore IV.
231 In the MIP test, specimens were first evacuated via heating inside a sealed penetrometer. Through
232 incremental hydraulic pressure, mercury was then progressively introduced into the specimens. The applied
233 pressure, *p* (MPa), and the volume of mercury intruded were registered progressively (Romero and Simms,
234 2008). Pore diameter, *D* was obtained according to the Washburn equation (Equation 2):

$$D = \frac{4.\gamma.\cos\theta}{\mathrm{p}} \qquad (2)$$

D is the diameter of the entrance pore where mercury intrudes, γ is the surface tension of mercury, and θ represents contact angle.

In this study, pore classifications were made as per the International Union of Pure and Applied Chemistry (IUPAC) (Rouquerol et al., 1994), which classifies pores based on their pore-width as macropores (> 500 Å), mesopores (20-500 Å), and micropores (< 20 Å).

The following nomenclatures are referred to for specimens' identifications: type of specimen (untreated, 1%/2.5%/4% lime-treated)-compaction mode (S/K)-type of permeant solutions (DW/LW). For example, 1%-S-DW represents 1% lime-treated statically compacted soil submitted to DW percolation.

3. Results

3.1. Comparative evaluation of UCS in the lime-treated unleached and leached soil

The UCS obtained from the lime-treated 28 days cured specimens (unleached) were compared with the UCS obtained from the lime-treated leached soil at the end of the hydraulic conductivity test (Fig. 2). The testing conditions during UCS test for each specimen were kept similar.

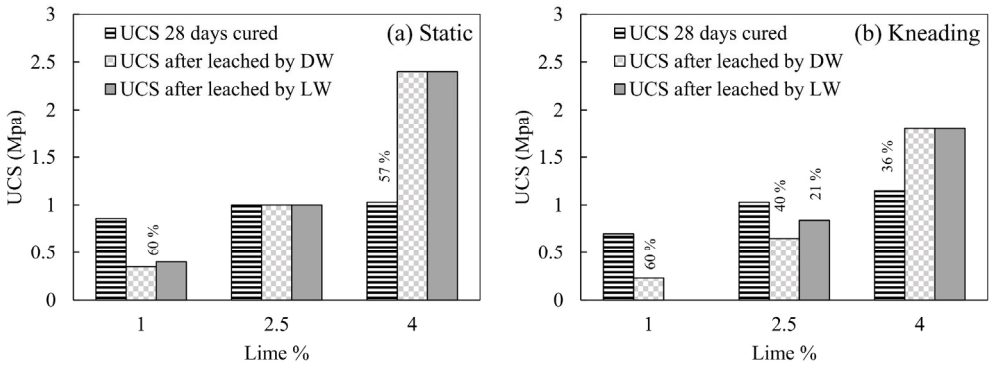

Fig. 2 Comparative evolution in UCS obtained in the 28 days cured and leached statically (a) and Kneading (b) compacted specimens

Fig. 2a shows that 1% lime-treated statically compacted specimens lost about 60% of the initial UCS on being leached by DW and LW. On the other hand, no significant change in the UCS was observed in the 2.5% lime-treated leached specimens. However, the UCS increased by about 57% for the 4% lime-treated leached specimens.

The UCS of 1% lime-treated kneaded specimens leached by DW decreased by about 60% (Fig. 2b). The UCS measurement of the corresponding LW submitted soil was not possible as the specimen broke at the end of the hydraulic conductivity test. About 40% of the initial UCS was lost in the 2.5% lime-treated DW leached kneaded specimen, whereas this decrease in UCS was about 20% in the corresponding LW leached specimen. The UCS for 4% lime-treated leached specimens increased by about 36%.

3.2. Comparative evolution of Pore size distribution

3.2.1. In 28-days cured lime-treated specimens

The Pore Size Distribution (PSD) of the statically and kneading compacted lime-treated 28-days cured specimens is summarized in Fig. 3.

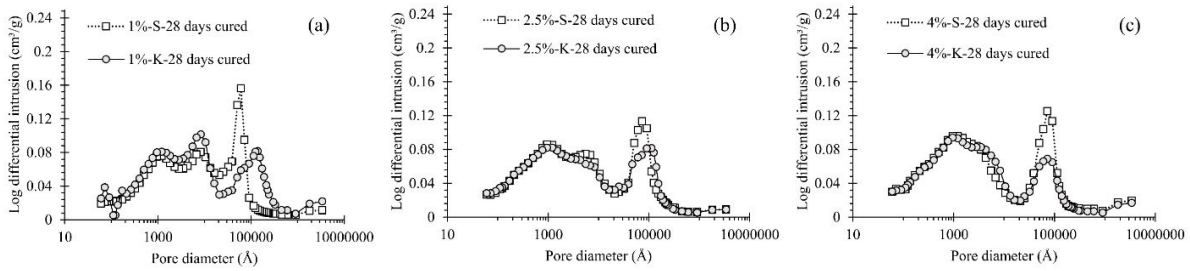

Fig. 3 Comparative evolution of PSD in the 1% (a), 2.5% (b), and 4% (c) lime-treated statically and Kneading compacted 28-days cured specimens

Three different peaks were observed at pore diameter 10^3, 10^4, and 10^5 Å. The total pores of diameter 10^3 Å were minimum in 1% lime-treated soil (Fig. 3a), slightly higher in 2.5% lime-treated soil (Fig. 3b), and maximum in 4% lime-treated soil (Fig. 3c). At the same time, pores of diameter 10^4 Å were minimum in 4% lime-treated soil and maximum in 1% lime-treated soil. This difference in the evolution of pores is attributed to the lime content used. At higher lime content, the evolution of cementitious compounds was enhanced (Lemaire et al., 2013; Little, 1987; Verbrugge et al., 2011), and hence more pores of diameter 10^3 Å were developed. The trend of pore evolution of diameters 10^3 and 10^4 Å remained at a similar level in both types of compacted soil.

However, the presence of the macropores of diameter 10^5 Å was comparatively significant in all the statically compacted specimens than the corresponding kneaded soil.

3.2.2. In unleached and leached lime-treated specimens

At the end of the hydraulic conductivity test, the evolution of PSD in the two types of compacted soil after being leached by DW and LW was compared with the unleached specimens in Fig. 4.

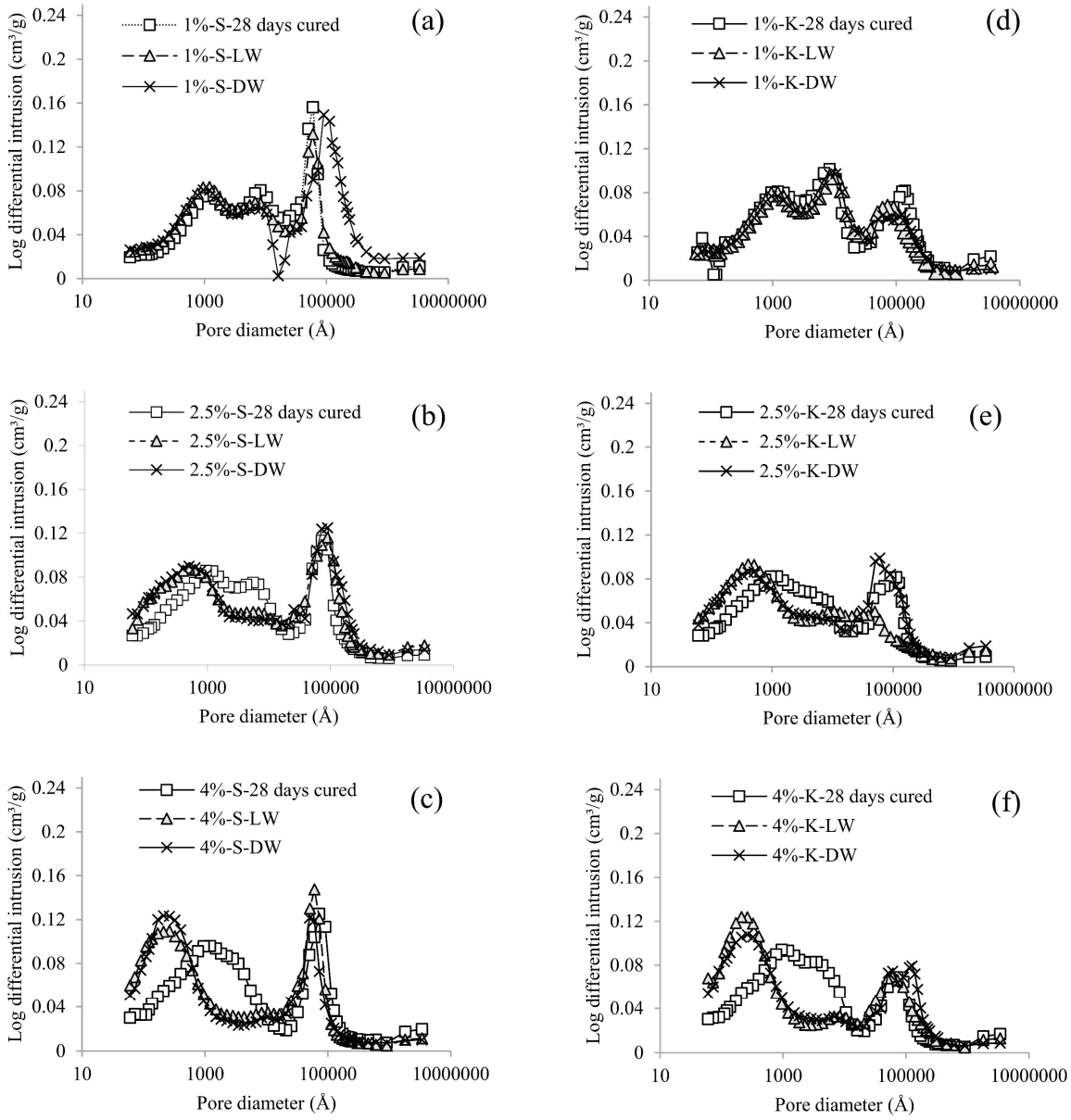

Fig. 4 Comparative evolution of PSD between 1%, 2.5%, and 4% lime-treated unleached and leached statically compacted (a-c) and kneading compacted specimens (d-f).

A decrease in the pores of diameter 10^4 Å and generation of pores of diameter lower than 10^3 Å in the 2.5% and 4% lime-treated leached specimens was observed compared to the unleached specimens (Fig. 4b, c, e & f). This generation of pores lower than 10^3 Å was relatively significant in the 4% lime-treated soil.

However, the macropores of diameter 10^5 Å increased in the 1% lime-treated statically compacted specimen after being leached by DW (Fig. 4a). At the same time, no significant change occurred in the corresponding LW leached specimen compared to the unleached specimen. In the 2.5% and 4% lime-treated soil, the evolution of macropores of diameter 10^5 Å remained constant after being leached by both DW and LW (Fig. 4b & c).

In the kneaded specimens, a constant evolution of the macropores of diameter 10^5 Å was observed in the leached and unleached 1% lime-treated specimens (Fig. 4d). On the other hand, the 2.5% lime-treated specimens showed an increase in the total 10^5 Å diameter macropores after being leached by DW, whereas in the corresponding LW submitted specimen, the total macropores with a similar diameter decreased and were lower than that of the unleached soil (Fig. 4e). In the 4% lime-treated soil, the total macropores with a diameter of 10^5 Å increased slightly in the DW leached specimen, while the total of this macropore feature remained almost constant in the corresponding LW leached specimen (Fig. 4f).

3.3. Hydraulic conductivity measurements in untreated and lime-treated soil

The analysis of the hydraulic conductivity was conducted after verifying the level of saturation in the lime-treated 28 days cured soils and at the end of the hydraulic conductivity test, *i.e.*, on completion of the renewal of 40 PVF. The measured degree of saturation, S_r is summarized in Table 3.

Table 3:

S_r measured in the lime-treated soil at the end of curing time and at the end of hydraulic test

	S_r (%) of statically compacted soil			S_r (%) of kneaded soil		
	1% lime-treated	2.5% lime-treated	4% lime-treated	1% lime-treated	2.5% lime-treated	4% lime-treated
After 28 days of curing	74.6	78.5	74.4	74.4	69.3	71.7
After 40 PVF was renewed in DW submitted soil	98.2	100	99.8	100	90.2	98.8
After 40 PVF was renewed in LW submitted soil	100	99.4	100	_	100	98.8

The S_r of all the 28 days cured lime-treated soils were less than 80%. This saturation level reached a value greater than 90%, when measured at the end of the hydraulic conductivity test. This difference in saturation values indicates that the hydraulic conductivity measurement was conducted in saturated specimens. It is worth noting that in-situ lime-treated soil may rarely reach a similar saturation level as the one obtained herein (Table 3) before the percolation happens.

The evolution in the *k* of the lime-treated and the untreated soil is presented in Fig. 5 with respect to the PVF measured during the hydraulic conductivity test.

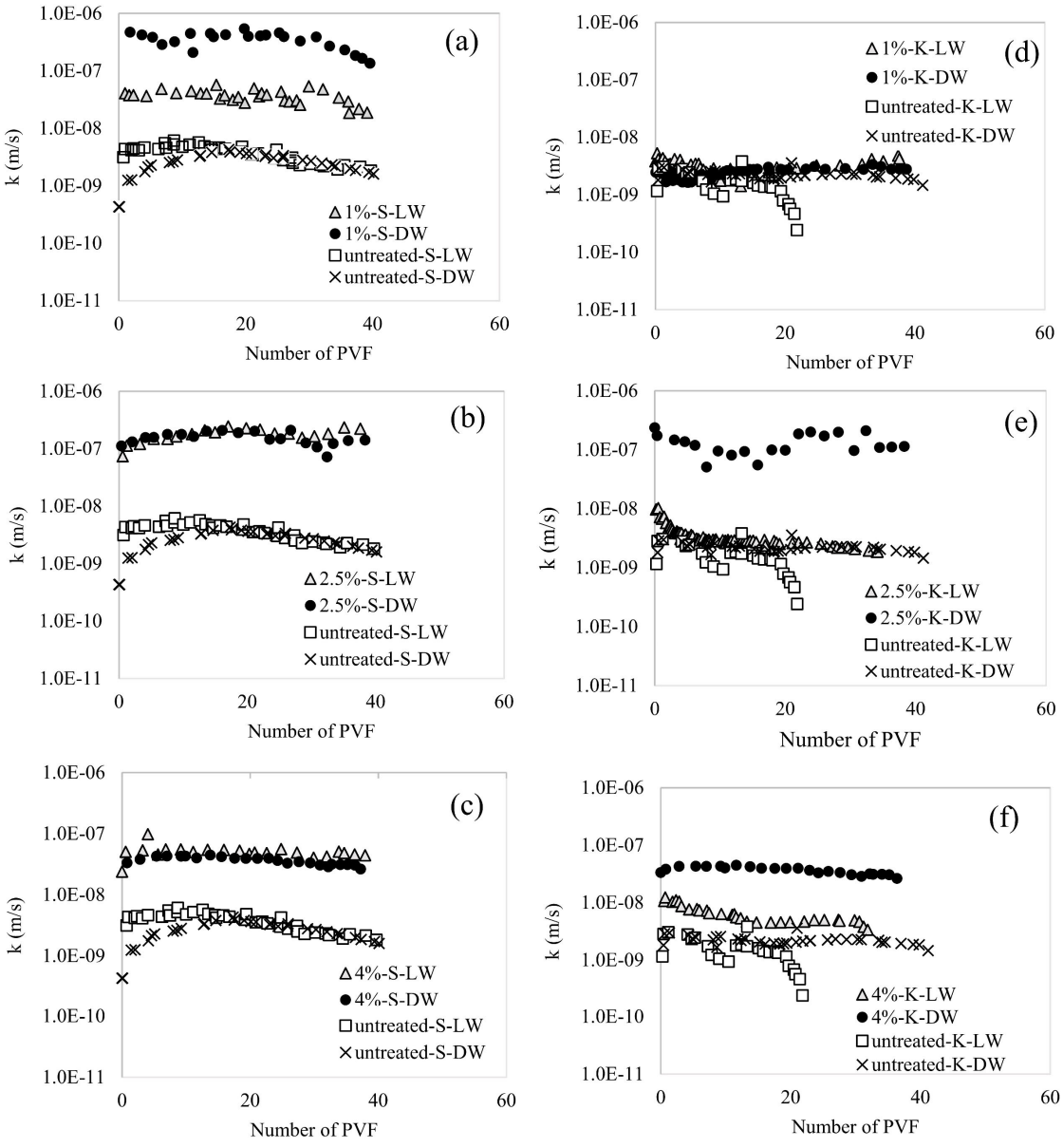

Fig. 5 Evolution in hydraulic conductivity of untreated and 1%, 2,5%, and 4% lime-treated DW and LW submitted statically (a-c), and kneading (d-f) compacted specimens

The duration taken by each specimen of the present dimensions to renew the volume of solution that corresponds to 40 PVF is provided in Table 4.

330

331 **Table 4:**

332 Duration of percolation phase in the lime-treated soil to renew 40 PVF of solutions

	Duration taken by statically compacted soil (days)				Duration taken by kneaded soil (days)			
	untreated	1% lime-treated	2.5% lime-treated	4% lime-treated	untreated	1% lime-treated	2.5% lime-treated	4% lime-treated
DW submitted soil	77	0.7	1.5	5	87	70	4	6
LW submitted soil	55	6	1.5	5	93	65	75	40

333

334

335 Fig. 5a shows that the magnitude of *k* in the untreated statically compacted specimens, submitted
336 to both types of solutions remained within the range of 10^{-8} to 10^{-9} m/s. This *k* then increased by about one
337 and two orders of magnitude in the 1% lime-treated LW and DW submitted soil, respectively. The duration
338 taken by the LW submitted soil to renew 40 PVF was about 5 days higher than the corresponding DW
339 submitted soil (Table 4). However, it took about 49 to 76 more days to circulate a similar volume of
340 solutions through the untreated soil.

341 In the 2.5% and 4% lime-treated statically compacted soil, the *k* was in between 10^{-7} to 10^{-8} m/s for
342 both DW and LW submitted soil. Thus, *k* was about one order of magnitude higher than the untreated soil
343 (Fig. 5b & c). The total duration corresponding to the percolation of 40 PVF was only 1.5 and 5 days for
344 the 2.5% and 4% lime-treated soil, respectively, which was much lower than the duration taken by the
345 corresponding untreated soil (Table 4).

346 For the lime-treated kneading compacted soil, the level of *k* measured for the untreated soil was in
347 the range of 10^{-8} to 10^{-9} m/s (Fig. 5d). In the untreated LW submitted soil, the level of *k* further decreased
348 after about 20 PVF. This decrease is attributed to the grain rearrangement within the soil matrix during the
349 percolation phase (Young, 2012). However, the obtained level of *k* in the 1% lime-treated kneaded
350 specimens submitted to DW and LW remained almost at a similar level as the untreated soil (Fig. 5d). At
351 the same time, the *k* increased by an order of magnitude in the 2.5% and 4% lime-treated kneaded specimen
352 submitted to DW, whereas it remained constant for the corresponding LW submitted specimen (Fig. 5e &
353 f). The 2.5% and 4% lime-treated kneaded soil took 75 and 40 days, respectively, to renew 40 PVF, whereas
354 the corresponding DW submitted soil took only 4-6 days to circulate the similar volume of solutions (Table
355 4). However, the duration of the percolation phase was relatively higher in the untreated kneaded soil than
356 in the lime-treated kneaded soil.

357 Based on the evolution of *k* obtained for each specimen in Fig. 5, Table 5 presents the estimated
358 hydraulic life expectancy of an in-situ lime-treated earth structure of a unit reference height if built with the

present soil configuration. The duration of life expectancy was expressed both in years and days (Column D) and was calculated by dividing the reference unit height of the structure by the average of the last 10 values of *k* measured in each specimen (Fig. 5).

As per Table 5, the estimated hydraulic life expectancy was 14.5 years for 2.5% lime-treated kneaded soil percolated by LW (Column D), while it was just 1.1 years for the corresponding DW percolated soil. For the 4% lime-treated soil, the life expectancy of the LW percolated sample was 6 years higher than that of the DW percolated sample. The difference in life expectancy based on the types of solution percolated was less significant for the 1% lime-treated kneaded soil. In the statically compacted soil, the difference in life expectancy for soil treated with 2.5% and 4% lime and percolated by both types of the solution was less significant. However, the hydraulic life expectancy of 1% lime-treated soil percolated by LW was 0.9 years higher than the corresponding DW percolated soil. It is worth noting that the above-estimated life expectancy did not consider the soil structure-pore fluid interactions during percolation. The obtained duration represents the duration taken by a given pore fluid to reach the bottom of a unit height structure if percolated from the top, considering *k* as the flow velocity.

Table 5:

Estimated life expectancy of a unit height in-situ earth structure, if built with the present soil configurations

A	B	C	D	E
Compaction modes	Specimen's configuration	Average *k* (m/s)	Estimated life expectancy for a unit height structure (years (days))	Required duration to reach 40 PVF in a unit height structure (days)
Statically compacted	1-S-OMC-28-DW	2.97E-07	0.1 (39.0)	16
	1-S-OMC-28-LW	3.30E-08	1.0 (350.6)	120
	2.5-S-OMC-28-DW	1.71E-07	0.2 (67.7)	32
	2.5-S-OMC-28-LW	2.01E-07	0.2 (57.7)	32
	4-S-OMC-28-DW	4.56E-08	1.0 (254)	100
	4-S-OMC-28-LW	4.73E-08	0.7 (244.7)	100
Kneading compacted	1-K-OMC-28-DW	2.91E-09	10.9 (3983.5)	1400
	1-K-OMC-28-LW	3.56E-09	8.9 (3249.4)	1300
	2.5-K-OMC-28-DW	1.49E-07	0.2 (77.7)	80
	2.5-K-OMC-28-LW	2.18E-09	14.5 (5297.0)	1500
	4-K-OMC-28-DW	3.00E-08	1.1 (385.8)	120
	4-K-OMC-28-LW	4.54E-09	7.0 (2548.3)	800

Each hydraulic conductivity test subjected specimens of given configuration took different durations to renew 40 PVF (Table 4). This duration was used to calculate the required duration to renew 40 PVF in a unit height hydraulic structure (Table 5, Column E). These obtained durations were further expressed in percentage with respect to the percentage of the total life expectancy estimated for the structure of unit height (*i.e.,* Column E/Column D) in Fig. 6.

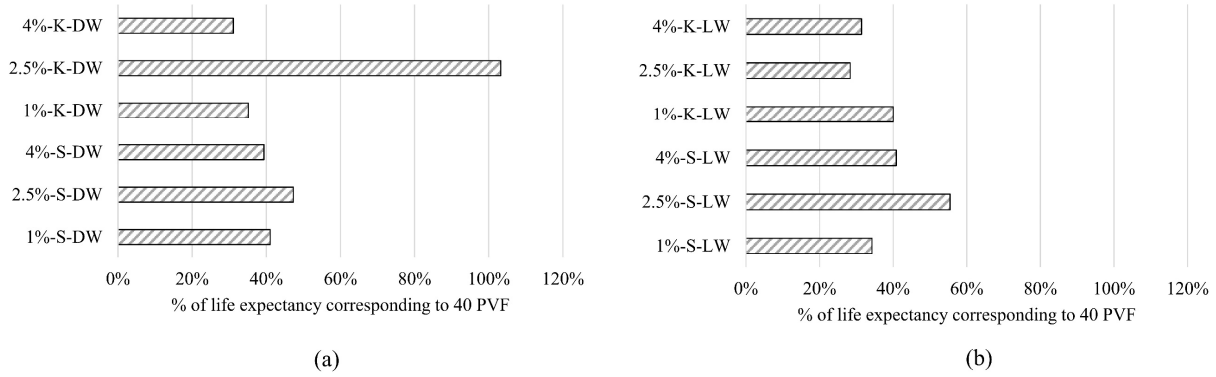

Fig. 6 Percentage of life expectancy that can be reached in a unit height earth structure if subjected to 40 PVF of DW (a) and LW (b) in kneading-and statically-compacted soil

According to Fig. 6a, the estimated lifetime of the 2.5% lime-treated kneaded soil structure, if percolated by 40 PVF of DW, has reached its expected life values. The corresponding kneaded specimen on being submitted to 40 PVF of LW reached only 28% of its total life expectancy (Fig. 6b). Besides, the renewal of 40 PVF has reached about 30 to 50% of the total estimated life of the structure, built with the remaining configuration. The above evaluation of hydraulic performance was in terms of PVF, which presents the advantage of considering the pore fluid-soil structure interactions. Based on this evaluation, it was shown that the total life expectancy was yet to be reached even after the renewal of 40 PVF (Fig. 6). Thus, such an assessment helps to investigate the life scale of in-situ earth structures at laboratory scale.

However, it is worth noting that the above estimation of life expectancy was based on the hydraulic performances and did not consider the mechanical performances of the compacted soil.

3.4. Evolution of calcium concentrations in the effluents of untreated and lime-treated soils

Fig. 7 presents the calcium concentration, *Ca* (mg/l) measured in the effluents collected at different PVF from the untreated and the lime-treated statically and kneaded specimens during the percolation phase.

405

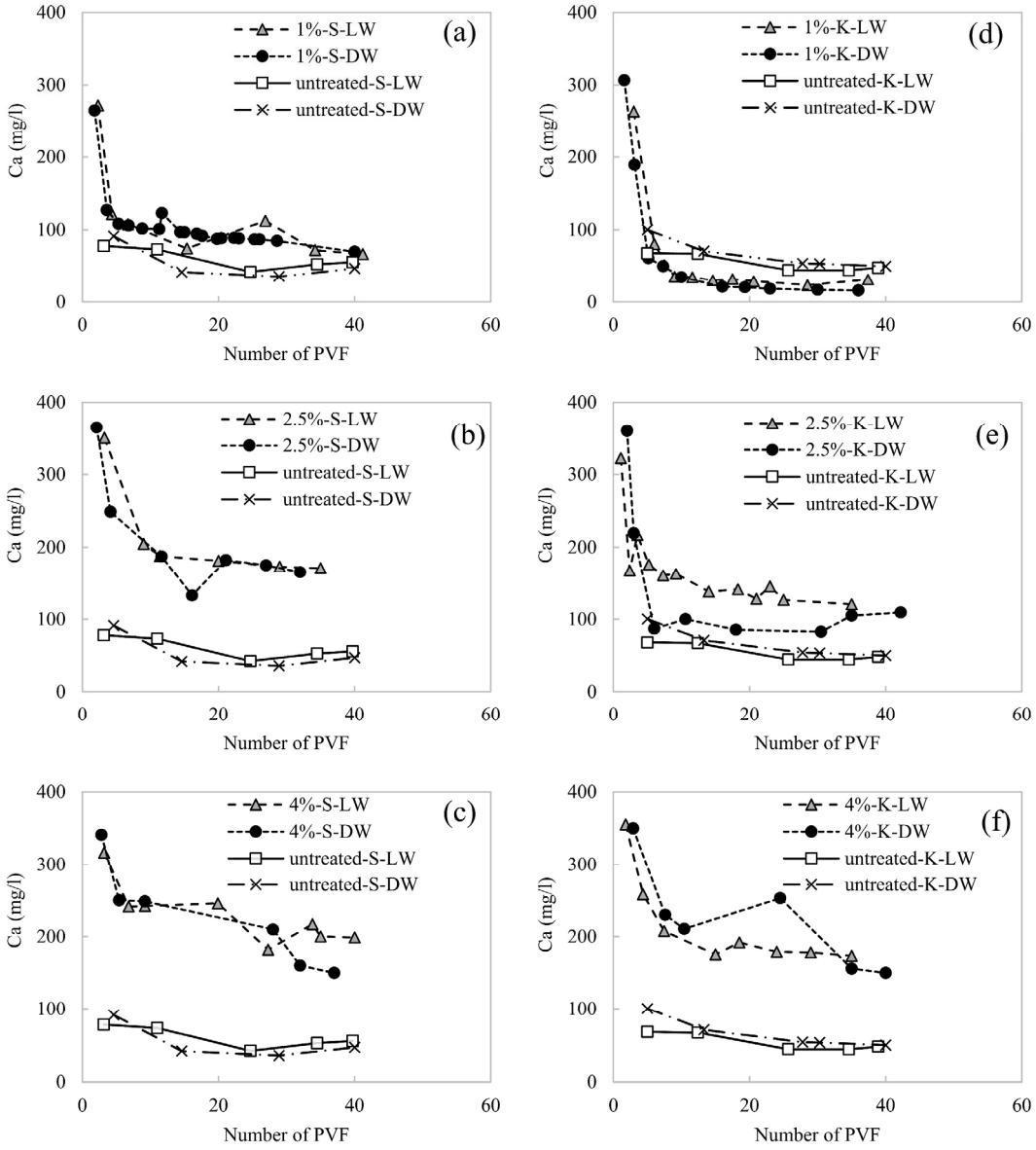

406

407 **Fig. 7** Concentration of *Ca* leached from the untreated and 1%, 2.5%, and 4% lime-treated DW & LW submitted statically (a-c)
408 and kneading (d-f) compacted specimens

409 Permeant solution flows mostly through the widest connecting pore available in soil (Hunt and
410 Sahimi, 2017). Hence, the leaching mechanism in a saturated lime-treated soil (Table 3) is more likely to
411 be pronounced on the available minerals around the inter-aggregate pores constituting the flow-path
412 compared to the intra-aggregate pores.

413 In the 1% lime-treated statically compacted soil, most of the *Ca* from the available and added lime,
414 particularly around the flow-path, was lost on renewal of 10 PVF of DW and LW (Fig. 7a). Further renewal

of solution triggered a release of soluble *Ca* from the soil. In the 2.5% and 4% lime-treated specimens, a sharp concentration of *Ca* was leached up to about 10 PVF, and the rate of leaching then slowed down. However, the overall trend of *Ca* leaching for the treated soil remained much above the trend obtained from the untreated soil, thus, indicating that the loss of *Ca* was either from the cementitious compounds or residual lime available, particularly the available *Ca* around the flow path (Fig. 7b & c).

For the kneading compacted soil, *Ca* available around the flow-path in the form of cementitious compounds or residual lime was lost completely at about 5-7 PVF from the 1% lime-treated soil (Fig. 7d). Then a concentration of soluble *Ca* was leached from the soil. The 2.5% lime-treated DW submitted specimen leached a significant *Ca* concentration, particularly coming from the lime added during the renewal of 40 PVF of DW. Besides, a part of soluble *Ca* was also lost from the soil (Fig. 7e). At the same time, the trend observed in the loss of *Ca* concentration in the corresponding LW submitted soil remained above the DW submitted soil, thus, indicating a part of *Ca* was lost only from the added lime (Fig. 7e).

For the 4% lime-treated kneaded soil, the evolution in the loss of *Ca* for the DW and LW submitted specimens remained at about a similar level (Fig. 7f). The leached *Ca* comes from the added lime.

Besides, the 2.5% and 4% lime-treated DW submitted kneaded soil leached a significant *Ca* concentration in just 4 and 6 days of percolation phase, respectively, whereas it took 75 and 40 days for the corresponding LW submitted soil to leach the equivalent *Ca* concentration (Table 4).

4. Discussions

4.1. Influence of pore fluid-soil structure interaction on the UCS evolution of lime-treated soil

Soil treated at LMO was shown to have a limited contribution towards the development of cementitious compounds (le Runigo et al., 2011). Hence, the addition of 1% lime to soil can be considered insufficient to maintain its strength and lost almost 60% of its initial UCS, irrespective of the compaction modes and the pore solutions the specimens were submitted to (Fig. 2).

The evolution of compressive strength in lime-treated soil enhances with the development of cementitious bonding, which depends on the lime content used (higher than the LMO), water content, and curing time (Das et al., 2020; Lemaire et al., 2013; Little, 1995; Verbrugge et al., 2011). Thus, in the 2.5% and 4% lime-treated soil, due to the constant contact of the compacted soil structure with the pore solution, particularly during the saturation phase, a significant evolution of cementitious compounds occurred. This was confirmed by the decrease in the total pores with a diameter of 10^4 Å, which in turn increased the formation of pores with a diameter lower than 10^3 Å in both the 2.5% and 4% lime-treated compacted

448 samples (Fig. 4b-c, e-f). As expected, the evolution of pore with a diameter lower than 10^3 Å was more
449 pronounced in the 4% lime-treated soil due to the greater availability of lime than that of the 1% and 2.5%
450 lime-treated samples. As a result, the UCS of the 4% lime-treated soil increased by 57% and 36% in the
451 statically and kneaded specimens, respectively, at the end of the hydraulic conductivity test compared to
452 the 28 days cured specimens (Fig. 2a & b). The UCS remained unaffected in the 2.5% lime-treated statically
453 compacted soil (Fig. 2a); however, it decreased in the corresponding kneaded soil.
454 The decrease in UCS of the kneaded soil was about 20% higher in the DW submitted soil than the
455 LW submitted soil (Fig. 2b). This relatively significant decrease in UCS indicates the pronounced influence
456 of pore solution chemistry on the kneaded soil structure. These phenomena are detailed in the later sections,
457 which involve the mechanism of hydraulic conductivity and leaching as a result of the coupled influence
458 of soil structures and pore solutions.
459
460 *4.2. Influence of pore fluid-soil structure interaction on the hydraulic behavior of lime-treated soil*
461
462 The observed hydraulic performances in the lime-treated soil appear to be in accordance with the
463 microstructural modifications brought about by a coupled effect produced between the compacted soil
464 structure and the chemistry of the solutions.
465
466 *4.2.1. Influence of soil structure on the hydraulic conductivity evolution*
467 Transport of pore fluid through a compacted soil matrix was shown to follow the pore geometry
468 constituted by the widest connecting pores (Hunt and Sahimi, 2017). Besides, previous studies have
469 demonstrated that lime treatment increases the size of inter-aggregates pores due to flocculation, and as a
470 result, increases the magnitude of hydraulic conductivity compared to the untreated soil (Nguyen et al.,
471 2015; Tran et al., 2014). This explains the increased k from about 10^{-9} m/s to somewhere in between 10^{-6}
472 and 10^{-8} m/s in all the lime-treated statically compacted specimens (Fig. 5a-c).
473 However, according to Mitchell and McConnell, (1965), under kneading action, flocculated
474 particles in natural soil break and transform into more likely a dispersed structure. This statement was
475 confirmed in the lime-treated soil studied herein. The large inter-aggregates formed due to lime treatment
476 were relatively deformed during kneading compaction, and consequently, the macropores were reduced.
477 Fig. 3 shows the presence of a relatively lower number of 10^5 Å diameter macropores in all the lime-treated
478 kneaded soil compared to the corresponding statically compacted soil. Thus, the evolution of k remained
479 constant, *i.e.*, between 10^{-8} to 10^{-9} m/s in the 1% lime-treated kneaded soil submitted to both types of
480 solutions, as well as the 2.5% and 4% lime-treated kneaded specimens submitted to LW (Fig. 5d-f).

However, the magnitude of k for the 2.5% and 4% lime-treated DW submitted soil was between 10^{-7} and 10^{-8} m/s, which was one order of magnitude higher than the corresponding untreated and LW submitted soil (Fig. 5e & f). This difference in k was because of the effect of pore solution chemistry, which is explained in the later section.

4.2.2. Influence of soil structure on flow characteristics

From the preceding discussion, different evolutions of 10^5 Å diameter macropores were observed under different methods of densification (*i.e.*, static and kneading actions). Hence it will be interesting to evaluate the flow path of the permeant solutions through both types of compacted structures, which is measured by hydraulic tortuosity.

The hydraulic tortuosity, T is defined as the parameter that characterizes the heterogeneity in the flow path of the solution in a porous media (Srisutthiyakorn and Mavko, 2016). In this study, T was calculated using the Kozeny-Carman equation (Equation 3), which considers T as a function of the pore geometry (Allen and Sun, 2017). Results of T calculated for the static and kneading compacted specimens are summarized in Table 6.

$$T = \sqrt{\frac{\phi^3}{ckS^2}} \quad (3)$$

In Equation 3, k is the coefficient of permeability in m/s, ϕ is the porosity calculated from each specimen, c is the Kozeny constant assumed to be equal to 200 for calculation convenience, and S is the specific surface area in m^2/g measured with BET. The value of c was considered based on the plot provided by Allen and Sun, (2017), where c was shown to be a function of the porosity of the soil.

Table 6

Tortuosity calculated from statically and kneading compacted specimens

Specimen ID	k (m/s)	ϕ	S (m^2/g)	T	Specimen ID	k (m/s)	ϕ	S (m^2/g)	T
1%-S-DW	2.97E-07	0.38	13.16	2.32	1%-K-DW	2.91E-09	0.37	11.75	24.84
1%-S-LW	3.30E-08	0.35	12.02	6.81	1%-K-LW	3.56E-09	0.37	11.62	23.34
2.5%-S-DW	1.71E-07	0.38	19.78	2.04	2.5%-K-DW	1.49E-07	0.38	18.56	2.27
2.5%-S-LW	2.01E-07	0.39	18.42	2.08	2.5%-K-LW	2.18E-09	0.38	18.56	19.46
4%-S-DW	4.56E-08	0.38	22.93	3.36	4%-K-DW	3.00E-08	0.37	22.10	4.12
4%-S-LW	4.73E-08	0.37	23.73	3.12	4%-K-LW	4.54E-09	0.39	20.60	12.34

According to Table 6, almost all the statically compacted specimens showed a comparatively lower value of T than the corresponding kneaded specimens. Thus, the consequence of kneading action on reducing total macropores of diameter 10^5 Å by deforming the flocculated particles was reflected in the greater value of T obtained in the kneaded soil. Hence, it can be said that the kneaded soil structure experiences an intimate and longer contact with the permeant solution, and the pore fluid within the kneaded soil structure has greater accessibility towards the available lime. Such intimacy is favorable for the development of pozzolanic reaction, and consequently, a significant formation of cementitious compounds can occur in the pores. This benefit of kneading action was confirmed by the observed decrease in the amount of 10^5 Å diameter macropores in the 2.5% lime-treated LW submitted kneaded soil compared to the unleached soil (Fig. 4e). As a result, the estimated hydraulic life expectancy and the duration to renew 40 PVF of LW through a unit height in-situ kneaded structure was relatively longer than the one obtained using the reference standard method (Table 5).

Based on the above discussion, Fig. 8 presents a synthetic schematic diagram that elaborates the flow paths within the lime-treated statically and kneading compacted soil.

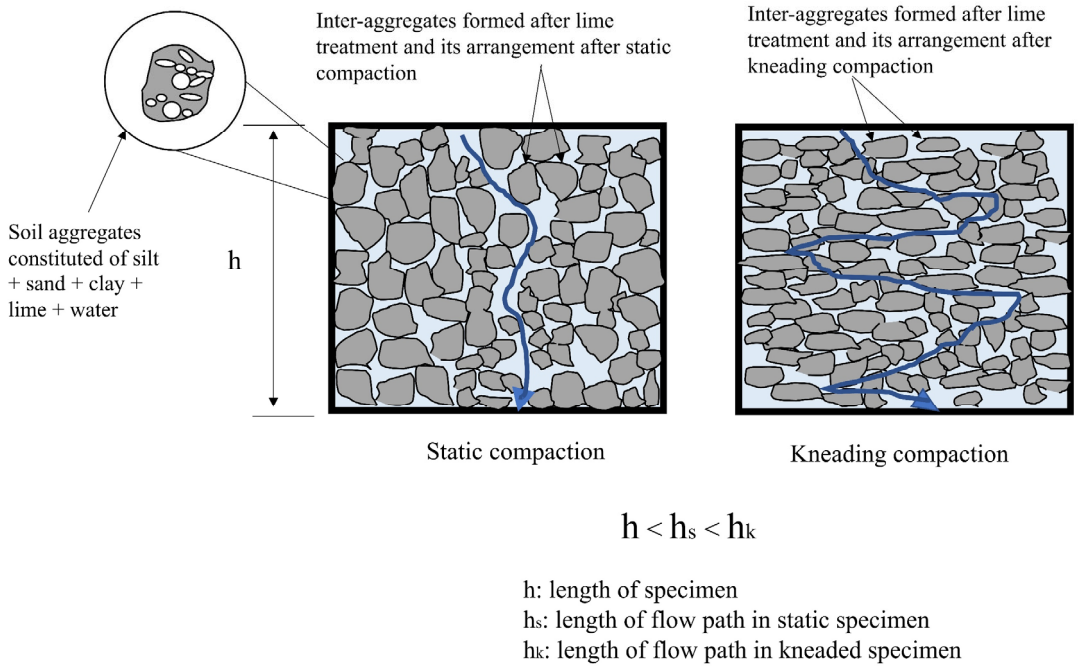

Fig. 8 Schematic diagram showing differences in lime-treated compacted soil matrices after being subjected to static and kneading compactions and the expected flow paths of permeant solution during hydraulic test

4.2.3. Influence of pore solution chemistry on flow characteristics and leaching mechanism

The mechanism of leaching was defined by the chemistry of the pore solutions the specimens were submitted to. As evident from Fig. 7e & f and Table 4, the leaching of *Ca* was comparatively higher and accelerated in the DW submitted kneaded specimens compared to the corresponding LW submitted specimens. As described earlier, due to the constant contact of soil-lime with the pore solution during the saturation phase of the hydraulic conductivity test, a significant formation of cementitious bonding occurred in the inter-and intra-aggregate pores. Once the percolation phase was initiated, the renewal of the pore solution occurred. Since DW is devoid of ions and has a low EC (Table 1), the DW dissolves a relatively significant quantity of *Ca* from the cementitious compounds, particularly those present around the flow path, and the soluble *Ca* from the soil. The dissolution of cementitious compounds from the macropores, thus, in turn, increased the magnitude of k (Fig. 5e & f). As a result, 40 PVF of DW was percolated through the 2.5% and 4% lime-treated kneaded soil only in 4 and 6 days, respectively. At the same time, the corresponding 2.5% and 4% lime-treated LW submitted specimens took 75 and 40 days, respectively, to percolate a similar volume of LW (Table 4). The above phenomena also explain the relatively significant UCS reduction observed in the DW submitted kneaded specimen (Fig. 2b).

However, the influence of pore solution chemistry in the leaching mechanism inducing a modification in the flow-path remained less pronounced in the 1% lime-treated kneaded specimen than in the 2.5% and 4% lime-treated samples. As soil treated at LMO has limited contribution towards the development of cementitious compounds, almost all *Ca* from the added lime was leached, and consequently, a significant amount of soluble *Ca* was leached from the soil (Fig. 7d). Besides, under the application of a constant load during kneading compaction, the flocculated particles in the 1% lime-treated specimens tend to deform more than the deformation of the 2.5% and 4% lime-treated soil as the addition of the higher lime dosages creates stronger flocculated particles. Thus, the evolution of k in the 1% lime-treated remained at a similar level as the untreated kneaded soil (Fig. 5d).

Although the impact of pore solution chemistry on the mechanical and hydraulic evolution was pronounced in the kneaded soil, it remained less significant in the statically compacted soil. Due to the presence of additional macropores (Fig. 3) in all the lime-treated statically compacted specimens, statically compacted soil can be said to have undergone preferential flow, which was reflected in the relatively lower value of T than that in the kneading compacted samples (Table 6). In the process of preferential flow, the pore solution-soil structure interaction remained less significant, and thus the leaching mechanism remained at a similar level irrespective of the types of pore solutions the specimens were submitted to (Fig. 7a-c). This explains the evolution of a similar level of k in the 2.5% and 4% lime-treated statically compacted soil regardless of the types of pore solution they were submitted to (Fig. 5b & c). It also explains the difference in UCS observed between the statically and kneading compacted soil (Fig. 2).

561 However, the *k* increased by 10 times in the 1% lime-treated DW submitted soil compared to the
562 LW submitted soil (Fig. 5a). Considering that the leaching mechanism in 1% lime-treated statically
563 compacted soil remained at a similar level (Fig. 7a), and 1% lime-treated soil has limited contribution
564 towards the deposition of cementitious compounds around the flow path; hence, the observed increase in
565 the *k* value in the DW submitted soil was due to the partial disintegration of inter-aggregates around the
566 flow path, which in turn increased the quantity of 10^5 Å diameter macropores (Fig. 4a).
567
568 *4.2.4. Comparison of hydraulic evolution in laboratory and in-situ cured soil*
569 The hydraulic evolution and the estimated hydraulic life expectancy of the 2.5% lime-treated LW
570 percolated kneaded soil (Table 5) were compared with the atmospherically cured specimens. In-situ
571 specimens were sampled from a 7-years atmospherically cured embankment built with the same soil
572 configuration, as reported by Das et al. (2020). The embankment was previously studied by Makki-
573 Szymkiewicz et al. (2015), who reported a *k* of 2.00E-09 m/s after 6 months of atmospheric curing. The
574 hydraulic conductivity was evaluated again after 7 years of atmospheric curing by subjecting the sample to
575 LW at the laboratory, and the *k* value was found to be 9.18E-10 m/s. The estimated hydraulic life expectancy
576 and the evolution of *k* in the laboratory and the in-situ cured specimens are compared and are presented in
577 Table 7.
578
579 **Table 7**
580 Comparison of *k* and life expectancy obtained for in-situ and laboratory cured 2.5% lime-treated kneaded soil, percolated by LW

Type of specimens	Duration of curing	*k* (m/s)	Life expectancy (years)
Laboratory-cured	28 days	2.18E-09	14.5
In-situ cured	6 months	2.00E-09	15.9
	7 years	9.18E-10	34.5

581
582 Table 7 shows that the obtained values of *k* and hydraulic life expectancy evolved in a positive
583 manner. The *k* value decreased while the hydraulic life expectancy increased with curing time. The decrease
584 in *k* was due to the evolution of cementitious compounds, which increased the mesopores by decreasing the
585 available macropores, as reported by Das et al. (2020). The increased mesopores positively contribute to an
586 increase in UCS, which has led to an average UCS of 3.29 MPa in the 7 years atmospherically cured soil,
587 as reported by Das et al. (2020).
588 Thus, in addition to the positive evolution of *k* with increased curing time, an enhanced mechanical
589 behavior can also be expected with time. Such an evolution can contribute to the increased hydromechanical

life expectancy of the structure. This underlines the relevance of kneading compaction and the use of LW to evaluate the long-term hydromechanical performance of lime-treated soil.

Conclusions

This study investigates the hydromechanical evolution in lime-treated soil based on the leaching mechanism and microstructural modifications brought about by a coupled pore solutions-soil structure interaction. Based on the analysis, the following conclusions are derived:

1) The evolution of UCS in the lime-treated leached specimens was impacted by combined influence created by (i) the availability of lime, (ii) the quality of the interaction of the pore fluid with the soil-lime component and, (iii) the impact of compaction mechanism on the extent of deformation of larger-sized flocculated particles. Thus, the UCS increased by 57% and 36% in the leached 4% lime-treated statically compacted and kneaded specimens, respectively, compared to the unleached specimens. The UCS remained unchanged in the 2.5% lime-treated statically compacted specimen, while it decreased by 21% and 40% in the 2.5% lime-treated kneaded soil, percolated by LW and DW, respectively.

2) Evaluation of hydraulic conductivity in terms of PVF helps to determine the percentage of life expectancy that can be reached in an in-situ hydraulic structure by considering the pore fluid-soil structure interactions. The renewal of 40 PVF corresponds to the deterioration of about 30 to 50% of the total estimated life of the lime-treated structure, built with the present soil configurations.

3) Kneading action reduced the number of macropores of diameter 10^5 Å in the compacted soil structure, which consequently reduces the magnitude of k. Thus, the magnitude of k was 10^{-8} to 10^{-9} m/s in the LW submitted kneaded soil, while it was 10^{-6} to 10^{-8} m/s in the corresponding statically compacted soil.

4) Higher hydraulic tortuosity obtained in the kneaded soil demonstrated the longer contact duration between the pore solution and the soil and lime component. This feature favored the development of cementitious compounds and lowered the macropores of diameter 10^5 Å in the 2.5% lime-treated LW submitted kneaded soil, which is favorable for the long-term performance of lime-treated earth structure.

5) The chemistry of pore fluid caused a significant modification in the hydromechanical evolution of lime-treated soil based on its accessibility to the soil and lime component. DW, being relatively more aggressive than LW, dissolved a significant amount of *Ca* from the cementitious compounds, thus resulting in an

increase in the k of 2.5% and 4% lime-treated kneaded soil. This influence of DW on the leaching mechanism and the hydraulic conductivity evolution remained less pronounced in the statically compacted soil than the kneaded soil due to the limited accessibility of pore fluid to the soil components.

6) The hydromechanical behavior of lime-treated kneaded soil evolved with curing time, which in turn increased the life expectancy of an in-situ earth structure. The hydraulic evolution and the life expectancy of 28 days laboratory cured 2.5% lime-treated kneaded soil, percolated by LW was 2.18E-09 m/s and 14.5 years, respectively. After 7 years of atmospheric curing, the hydraulic evolution and the life expectancy evolved to 9.18E-10 m/s and 34.5 years, respectively. Such observations were due to evolution of cementitious compounds, which also increased the UCS to 3.29 MPa. This underlines the relevance of the use of kneaded soil and LW to evaluate the long-term hydromechanical performance of the lime-treated in-situ structure.

7) Soil treated at LMO (1%) has limited contribution towards the development of cementitious compounds. Thus, the influence of pore solution-soil structure interaction remained less significant in the hydraulic, leaching, and compressive strength evolution of the 1% lime-treated soil, whereas significant modifications in these properties can be observed in soil treated with lime content of 2.5% and 4%.

Thus, the above findings showed that the hydromechanical evolution in lime-treated soil is governed by the mechanism created during the pore fluid-soil structure interactions. The duration of the pore fluid-soil structure interaction is defined by the compaction mechanism implemented, and the extent of influence is determined by the pore solution chemistry and the lime content added. Implementation of kneading compaction accompanied with 10^{-3} M of NaCl concentration, a low ionic strength solution brings a significant modification in the hydromechanical performance. Thus, the selected compaction procedure and the permeant solution in the laboratory scale must be representative of the compaction mechanism and pore water that the structure is likely to be subjected to in the field. This will help to have a close prediction of the long-term hydromechanical performance of in-situ lime-treated structures. Such a prediction can contribute effectively to the efficient management of construction resources. Besides, to have a considerable modification in the hydromechanical performance, the addition of lime content higher than LMO is essential.

Acknowledgements

This work was financially supported by Association Nationale de la Recherche et de la Technologie with grant N°2018/0219 and Lhoist Southern Europe with grant N°RP2-E18114. The authors are very thankful to the research team of Université Gustave Eiffel, and Lhoist Nivelle for their great support in performing laboratory experiments and technical supports.

References

Akula, P., Hariharan, N., Little, D.N., Lesueur, D., Herrier, G., 2020. Evaluating the Long-Term Durability of Lime Treatment in Hydraulic Structures: Case Study on the Friant-Kern Canal. Transportation Research Record 2674 (6), 431–443. https://doi. org/10.1177/0361198120919404.

Ali, H., Mohamed, M., 2019. Assessment of lime treatment of expansive clays with different mineralogy at low and high temperatures. Construction and Building Materials 228, 116955. https://doi.org/10.1016/j.conbuildmat.2019.116955

Allen, R., Sun, S., 2017. Computing and comparing effective properties for flow and transport in computer-generated porous media. Geofluids. https://doi.org/10.1155/2017/4517259

A. ASTM, D698-12e2 (2012), Standard Test Methods for Laboratory Compaction Characteristics of Soil Using Standard Effort (12 400 Ft-Lbf/Ft3 (600 KN-m/M3)). American Society for Testing and Materials, West Conshohocken, PA.

Bell, F.G., 1996. Lime stabilization of clay minerals and soils. Engineering geology 42, 223–237.

Charles, I., Herrier, G., Chevalier, C., Durand, E., 2012. An experimental full-scale hydraulic earthen structure in lime treated soil, in: 6th International Conference on Scour and Erosion, Paris. pp. 1223–1230.

Clegg, B., 1964. Kneading compaction. Australian Road Research Board Bulletin 1.

Cuisinier, O., Auriol, J.-C., le Borgne, T., Deneele, D., 2011. Microstructure and hydraulic conductivity of a compacted lime-treated soil. Engineering geology 123, 187–193. https://doi.org/10.1016/j.enggeo.2011.07.010

Das, G., Razakamanantsoa, A., Herrier, G., Saussaye, L., Lesueur, D., Deneele, D., 2020. Evaluation of the long-term effect of lime treatment on a silty soil embankment after seven years of atmospheric exposure: Mechanical, physicochemical, and microstructural studies. Engineering Geology 105986. https://doi.org/10.1016/j.enggeo.2020.105986.

686 Das, G., Razakamanantsoa, A., Herrier, G., Deneele, D., 2021. Compressive strength and microstructure
687 evolution of lime-treated silty soil subjected to kneading action. Transportation Geotechnics, 29,
688 100568. https://doi.org/10.1016/j.trgeo.2021.100568

689 Deneele, D., le Runigo, B., Cui, Y.-J., Cuisinier, O., Ferber, V., 2016. Experimental assessment regarding
690 leaching of lime-treated silt. Construction and Building Materials 112, 1032–1040.
691 https://doi.org/10.1016/j.conbuildmat.2016.03.015

692 Diamond, S., Kinter, E.B., 1965. Mechanisms of soil-lime stabilization. Highway Research Record 92,
693 83–102.

694 Dowling, A., O'Dwyer, J., Adley, C.C., 2015. Lime in the limelight. Journal of cleaner production 92,
695 13–22. https://doi.org/10.1016/j.jclepro.2014.12.047

696 Eades, J.L., Grim, R.E., 1966. A quick test to determine lime requirements for lime stabilization.
697 Highway research record.

698 He, J., Wang, Y., Li, Y., Ruan, X., 2015. Effects of leachate infiltration and desiccation cracks on
699 hydraulic conductivity of compacted clay. Water Science and Engineering 8, 151–157.
700 https://doi.org/10.1016/j.wse.2015.04.004

701 Holtz, R.D., Kovacs, W.D., Sheahan, T.C., 1981. An introduction to geotechnical engineering. Prentice-
702 Hall Englewood Cliffs, NJ.

703 Hopkins, T.C., Beckham, T.L., Sun, C., 2007. Stockpiling Hydrated Lime-Soil Mixtures.
704 http://dx.doi.org/10.13023/KTC.RR.2007.12

705 Houben, H., Guillaud, H., 1994. de l'article/du chapitre Earth construction. A comprehensive guide.
706 distributeur Craterre-Eag.

707 Hunt, A.G., Sahimi, M., 2017. Flow, transport, and reaction in porous media: Percolation scaling, critical-
708 path analysis, and effective medium approximation. Reviews of Geophysics 55, 993–1078.
709 https://doi.org/10.1002/2017RG000558

710 Inkham, R., Kijjanapanich, V., Huttagosol, P., Kijjanapanich, P., 2019. Low-cost alkaline substances for
711 the chemical stabilization of cadmium-contaminated soils. Journal of environmental management
712 250, 109395. https://doi.org/10.1016/j.jenvman.2019.109395

713 Katsumi, T., Ishimori, H., Onikata, M., Fukagawa, R., 2008. Long-term barrier performance of modified
714 bentonite materials against sodium and calcium permeant solutions. Geotextiles and Geomembranes
715 26, 14–30. https://doi.org/10.1016/j.geotexmem.2007.04.003

716 Kolias, S., Kasselouri-Rigopoulou, V., Karahalios, A., 2005. Stabilisation of clayey soils with high
717 calcium fly ash and cement. Cement and Concrete Composites 27, 301–313.
718 https://doi.org/10.1016/j.cemconcomp.2004.02.019

719 Kouassi, P., Breysse, D., Girard, H., Poulain, D., 2000. A new technique of kneading compaction in the
720 laboratory. Geotechnical testing journal 23, 72–82. https://doi.org/10.1520/GTJ11125J

721 le Runigo, B., Cuisinier, O., Cui, Y.-J., Ferber, V., Deneele, D., 2009. Impact of initial state on the fabric
722 and permeability of a lime-treated silt under long-term leaching. Canadian Geotechnical Journal 46,
723 1243–1257. https://doi.org/10.1139/T09-061

724 le Runigo, B., Ferber, V., Cui, Y.-J., Cuisinier, O., Deneele, D., 2011. Performance of lime-treated silty
725 soil under long-term hydraulic conditions. Engineering geology 118, 20–28.
726 https://doi.org/10.1016/j.enggeo.2010.12.002

727 Lemaire, K., Deneele, D., Bonnet, S., Legret, M., 2013. Effects of lime and cement treatment on the
728 physicochemical, microstructural and mechanical characteristics of a plastic silt. Engineering
729 Geology 166, 255–261. https://doi.org/10.1016/j.enggeo.2013.09.012

730 Little, D.N., 1995. Stabilization of pavement subgrades and base courses with lime.

731 Little, D.N., 1987. Fundamentals of the Stabilization of Soil with Lime. National Lime Association.

732 Makki-Szymkiewicz, L., Hibouche, A., Taibi, S., Herrier, G., Lesueur, D., Fleureau, J.-M., 2015.
733 Evolution of the properties of lime-treated silty soil in a small experimental embankment.
734 Engineering Geology 191, 8–22. https://doi.org/10.1016/j.enggeo.2015.03.008

735 Miller, G.A., Azad, S., 2000. Influence of soil type on stabilization with cement kiln dust. Construction
736 and building materials 14, 89–97. https://doi.org/10.1016/S0950-0618(00)00007-6

737 Mitchell, J.K., Hooper, D.R., Campenella, R.G., 1965. Permeability of compacted clay. Journal of the
738 Soil Mechanics and Foundations Division 91, 41–65.

739 Mitchell, J.K., McConnell, J.R., 1965. Some Characteristics of the elastic and plastic deformation of clay
740 on initial loading. Institute of Transportation and Traffic Engineering, University of California.

741 Nguyen, T.T.H., Cui, Y.J., Herrier, G., Tang, A.M., 2015. Effect of lime treatment on the hydraulic
742 conductivity of a silty soil.

743 Poh, H.Y., Ghataora, G.S., Ghazireh, N., 2006. Soil stabilization using basic oxygen steel slag fines.
744 Journal of materials in Civil Engineering 18, 229–240. https://doi.org/10.1061/(ASCE)0899-
745 1561(2006)18:2(229)

746 Pu, S., Zhu, Z., Wang, H., Song, W., Wei, R., 2019. Mechanical characteristics and water stability of silt
747 solidified by incorporating lime, lime and cement mixture, and SEU-2 binder. Construction and
748 Building Materials 214, 111–120. https://doi.org/10.1016/j.conbuildmat.2019.04.103

749 Ranaivomanana, H., Razakamanantsoa, A., Amiri, O., 2018. Effects of cement treatment on
750 microstructural, hydraulic, and mechanical properties of compacted soils: Characterization and
751 modeling. International Journal of Geomechanics 18, 04018106.
752 https://doi.org/10.1061/(ASCE)GM.1943-5622.0001248

753 Ranaivomanana, H., Razakamanantsoa, A., Amiri, O., 2017. Permeability prediction of soils including
754 degree of compaction and microstructure. International Journal of Geomechanics 17, 04016107.
755 https://doi.org/10.1061/(ASCE)GM.1943-5622.0000792

756 Razakamanantsoa, A.R., Djeran-Maigre, I., 2016. Long term chemo-hydro-mechanical behavior of
757 compacted soil bentonite polymer complex submitted to synthetic leachate. Waste management, *53*,
758 92-104. https://doi.org/10.1016/j.wasman.2016.04.023

759 Romero, E., Simms, P.H., 2008. Microstructure investigation in unsaturated soils: a review with special
760 attention to contribution of mercury intrusion porosimetry and environmental scanning electron
761 microscopy. Geotechnical and Geological engineering 26, 705–727.

762 Rouquerol, J., Avnir, D., Fairbridge, C.W., Everett, D.H., Haynes, J.M., Pernicone, N., Ramsay, J.D.F.,
763 Sing, K.S.W., Unger, K.K., 1994. Recommendations for the characterization of porous solids
764 (Technical Report). Pure and Applied Chemistry 66, 1739–1758.

765 Sato, K., Barast, G., Razakamanantsoa, A.R., Djeran-Maigre, I., Katsumi, T., Levacher, D., 2017.
766 Comparison of prehydration and polymer adding effects on Na activated Ca-bentonite by free swell
767 index test. Applied Clay Science 142, 69–80. https://doi.org/10.1016/j.clay.2016.10.009

768 Shackelford, C.D., Benson, C.H., Katsumi, T., Edil, T.B., Lin, L., 2000. Evaluating the hydraulic
769 conductivity of GCLs permeated with non-standard liquids. Geotextiles and Geomembranes 18,
770 133–161. https://doi.org/10.1016/S0266-1144(99)00024-2

771 Show, K.-Y., Tay, J.-H., Goh, A.T.C., 2003. Reuse of incinerator fly ash in soft soil stabilization. Journal
772 of materials in civil engineering 15, 335–343. https://doi.org/10.1061/(ASCE)0899-
773 1561(2003)15:4(335)

774 Srisutthiyakorn, N., Mavko, G., 2016. Hydraulic tortuosity: From artificial packs to natural rocks, in:
775 SEG Technical Program Expanded Abstracts 2016. Society of Exploration Geophysicists, pp. 3133–
776 3137. https://doi.org/10.1190/segam2016-13966753.1

777 Sunil, B.M., Shrihari, S., Nayak, S., 2008. Soil-leachate interaction and their effects on hydraulic
778 conductivity and compaction characteristics, in: 12th International Conference on Computer
779 Methods and Advances in Geomechanics. pp. 2380–2386.

780 Tran, T.D., Cui, Y.-J., Tang, A.M., Audiguier, M., Cojean, R., 2014. Effects of lime treatment on the
781 microstructure and hydraulic conductivity of Héricourt clay. Journal of Rock Mechanics and
782 Geotechnical Engineering 6, 399–404. https://doi.org/10.1016/j.jrmge.2014.07.001

783 Vaverková, M.D., Elbl, J., Koda, E., Adamcová, D., Bilgin, A., Lukas, V., Podlasek, A., Kintl, A.,
784 Wdowska, M., Brtnický, M., 2020. Chemical Composition and Hazardous Effects of Leachate from
785 the Active Municipal Solid Waste Landfill Surrounded by Farmlands. Sustainability 12, 4531.
786 https://doi.org/10.3390/su12114531

787 Verbrugge, J.-C., de Bel, R., Correia, A.G., Duvigneaud, P.-H., Herrier, G., 2011. Strength and micro
788 observations on a lime treated silty soil, in: Road Materials and New Innovations in Pavement
789 Engineering. pp. 89–96. https://doi.org/10.1061/47634(413)12

790 Watabe, Y., Leroueil, S., le Bihan, J.-P., 2000. Influence of compaction conditions on pore-size
791 distribution and saturated hydraulic conductivity of a glacial till. Canadian Geotechnical Journal 37,
792 1184–1194. https://doi.org/10.1139/t00-053

793 Wild, S., Kinuthia, J.M., Jones, G.I., Higgins, D.D., 1998. Effects of partial substitution of lime with
794 ground granulated blast furnace slag (GGBS) on the strength properties of lime-stabilised sulphate-
795 bearing clay soils. Engineering Geology 51, 37–53. https://doi.org/10.1016/S0013-7952(98)00039-8

796 Young, R., 2012. Soil properties and behaviour. Elsevier.

797